On The Accurate Calibration of The SeaWinds Radar Antenna: A Cylindrical Near-Field Measurement Approach

Ziad A. Hussein[1,2] and Yahya Rahmat-Samii[2,1]

[1]Jet Propulsion Laboratory
California Institute of Technology
Pasadena, California 91109

[2]University of California Los Angeles
Los Angeles, CA 90024-1594

Abstract

A multipolarization, multi-incidence angle conical scanning Ku-band radar antenna is currently being designed and calibrated at the Jet Propulsion Laboratory (JPL) for the SeaWinds Scatterometer instrument. To calibrate the radar's performance, it is essential to accurately determine the antenna gain and radiation pattern characteristics over wide angular range. Such characterizations may be performed on a far-field range or in an indoor near-field measurement facility. Among the advantage of the latter is that the antenna is in a controlled environment. This paper demonstrates the utility of a cylindrical near-field measurement approach for the SeaWinds radar antenna calibration. Both generalized measurement error models and measured tests on a standard gain horn and NASA Scatterometer instrument antenna have been performed to achieve and verify the desired calibration accuracy. A comparison between far-field measured data and those obtained from cylindrical near-field measurements was found in excellent agreement.

1. Introduction

Recent spaceborne scatterometers demand very high quality performance from radar antennas. For example, a recently designed JPL/NASA SeaWinds spaceborne scatterometer for global mapping of dynamic change of ocean circulation requires accurate knowledge of antenna gain, wide-angle antenna patterns, pointing, and beamwidth. The antenna assembled on this instrument is an elliptical parabolic reflector with two independent beams pointing at 40 and 46 degrees from nadir to provide a cross track measurement range of 900 km. The inner beam (40 degrees from nadir) is a horizontal polarization, H-pol, with 1.6 x 1.8 degrees beamwidth in elevation and azimuth plane respectively. The outer beam (46 degrees from nadir) is a vertical polarization, V-pol, with 1.4 x 1.7 degrees beamwidth. The instrument operates at Ku-band. 13.402 GHz.

Near-field measurement has been used for many years to determine the far-field radiation patterns of antennas with high accuracy [1]. In order to accurately characterize the radiation performance of SeaWinds radar antenna at JPL, a cylindrical near-field measurement facility has been developed (Figure 1). It is the objective of this paper to present a cylindrical near-field calibration approach with generalized measurement error models to properly determine the effect of near-field bias errors on antenna gain and far-field radiation patterns, and to critically assess the importance of different error mechanisms in evaluating the achievable accuracy in absolute gain and pattern measurements.

The following is a description of the cylindrical near-field measurement set up at J PI,, error analysis technique, a verification of the calibration accuracy with the use of standard gain horn measurement in the cylindrical near-field at 13.402 GHz with those

measured at National Institute of Standard and Technology (NISI') in the far-field range, and the SeaWinds radar antenna comparative performance with those measured in the far-field range.

2. Cylindrical Near-Field Measurement Implementation

The cylindrical near-field measurement facility at JPL, shown in Figure 1, is implemented such that the sampling orthomode probe steps along the vertical direction (3.8 meter long) and the antenna under test rotates in azimuth. The sampling probe measures the amplitude and phase tangential electric field components on a cylindrical surface enclosing the test antenna as illustrated in Figure 2. An RF switch at the input of the sampling probe is used to switch between the electric field components. In order to maintain the relative ratio between the measured field components, the insertion loss difference, amplitude and phase, of the RF switch is determined. This difference is corrected at the front panel of SA 1795 receiver. The antenna under test is then optically aligned to the probe coordinate system. Probe compensation is used to correct for the probe's radiation characteristics [2] including probe antenna gain, patterns and input reflection coefficients. The insertion loss between the antenna under test and the probe, normally taken at the peak of the near-field on the scanning cylindrical surface, is determined. The absolute antenna gain and far-field radiation patterns are then obtained via near-field to far-field transformation [2-4] .

3. Error Analysis

There arc two types of bias errors in near-field antenna calibration: electrical and mechanical. The electrical errors are dominated by the probe-antenna under test interaction, scan area truncation, receiver nonlinearity and drift, and probe gain and relative patterns. The mechanical errors, which may also induce bias errors in the calculated far-field radiation patterns, arc mainly probe position with respect to the center of the rotation of the antenna as it steps along the z-direction, probe orientation, and antenna under test alignment.

Probe tower alignment is critical to the prediction of the antenna pointing accuracy. Misalignment causes a pattern shift that is proportional to the slope of the tower. For example, it has been demonstrated with computer simulation that a 0.02-degree pointing error in elevation necessitates a probe-position alignment to better 1/16 wavelength.

Multiple reflections between the probe and the antenna will greatly affect antenna gain and relative pattern accuracy. Figure 3 depicts the deviations in far-field patterns computed from near-field data measured on successive cylindrical near-field surfaces separated by l/4. Near-field truncation along the Y.-direction will greatly affect the sidelobe level and angular location in the computed far field radiation patterns in elevation plane [4]. A near-field truncation error in the azimuth direction will deter our ability to predict the backlobe far-field patterns in that direction. It has been observed that the pattern accuracy deteriorates rapidly in azimuth, starting at an angle coinciding with the truncated angular near-field region. Accurate knowledge of the radial separation distance, r_o, between the AUT and the phase center of the probe is important to predict antenna gain and relative patterns. Figure 4 describes the relative change of antenna gain vs. radial error.

4. Standard Gain horn Antenna Results

A standard gain horn, SGH, model 12-12, has been employed to verify the cylindrical near-field measurement setup and accuracy. The SGH was measured in the cylindrical near-field range at SeaWinds radar antenna operating frequency 13.402 GHz. Far-field patterns and antenna gain were then computed. A comparison between the SGH antenna gain measured at NIST using a generalized three antenna measurement techniques [5] at the same frequency and those measured in the above described approach shows an excellent agreement (within O. 18 dB difference) as shown in Table 1.

Table 1. Comparison between SGH antenna gain measured at **NIST** and gain measured at JPL

JPL SGH Gain Measurement	NIST SGH Gain Measurement	Difference
23.98 dB	23.80 dB	0.18 dB

Furthermore, a comparison between direct far-field pattern measurement of the SGH at JPL's 3000-foot range and those constructed from cylindrical near-field measurement is shown in Figure 5. As can be seen, the results are in very good agreement down to 40 dB from the peak of the beam. It is worthwhile to note here that the 3000-foot far-field range has a limited dynamic range of 40 dB. This is evident in the far-field patterns shown in Figure 5 at an amplitude level below 40 dB from the peak.

5. SeaWinds Radar Antenna Results

The SeaWinds radar antenna horizontal and vertical polarization were measured in the cylindrical near-field range. The radar antenna performance parameters were then compared to those obtained in the JPL 's WOO-foot range. Figure 6 and 7 depict the radiation patterns of the antenna horizontal polarization in the elevation and azimuth plane respectively. It is seen that the results are in very good agreement. Similarly, the vertical polarization of the SeaWinds radar antenna was measured and compared to the results obtained in the direct far-field measurement in the elevation and azimuth plane as shown in Figure 8 and 9 respectively.

References

[1] Special Issue on Near-Field Scanning Techniques, *IEEE Trans.*, Antennas and Propagat., Vol. Ap-36, June 1988.

[2] Z.A. Hussein and Y. Rahmat-Samii, "Probe Compensation Characterization in Cylindrical Near-Field Scanning" *IEEE AP-S Symp. Digest*, Ann Arbor, Michigan, June 1993.

[3] A. D. Yaghjian, "Near-Field Antenna Measurement On A Cylindrical Surface: A Source Scattering-Matrix Formulation", *NBS Tech.* Note 696, July 1977.

[4] Z.A. Hussein, "Probe Compensation And Error Analysis In Cylindrical Near-Field Scanning" *16th Annual AMTA Symp. Digest*, Long Beach, CA, October 1994.

[5] A.C. Newell, R.C. Baird, and P.F. Wacker, "Acuurate Measurement Of Antenna Gain And Polarization At Reduced Distances By An Extrapolation Techniques", *IEEE Trans*, vol. AP-21, N04, pp. 418-431, July 1973.

Acknowledgment

This work was carried out at the Jet Propulsion Laboratory, California Institute of Technology, under contract with the National Aeronautics and Space Administration. The authors would like to thank Mr. K. Kellogg for his support and Mr. R. Thomas for his assistance in the measurement.

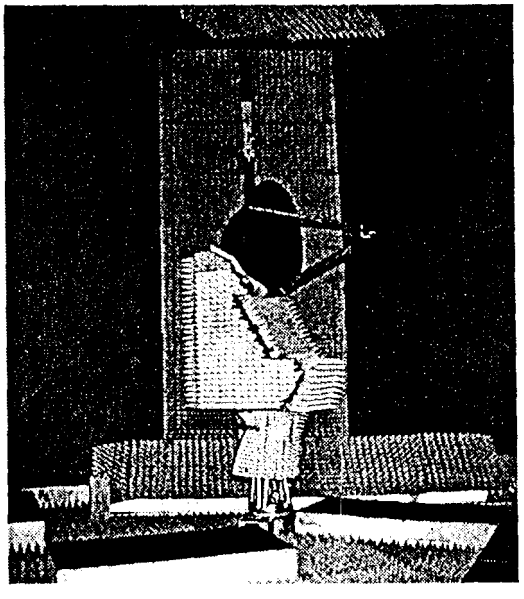

Figure 1. SeaWinds radar Antenna mounted in the cylindrical near-field range facility at the JPL.

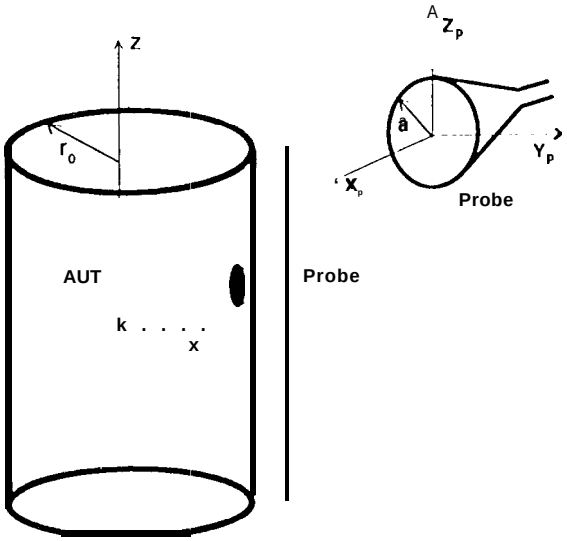

Figure 2. (a) Cylindrical near-field configuration and (b) probe coordinate system.

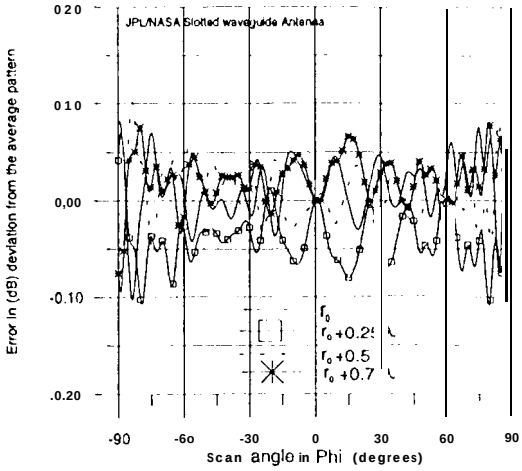

Figure 3. Typical far-field pattern error variation due to near-field multiple reflection between probe and antenna under test.

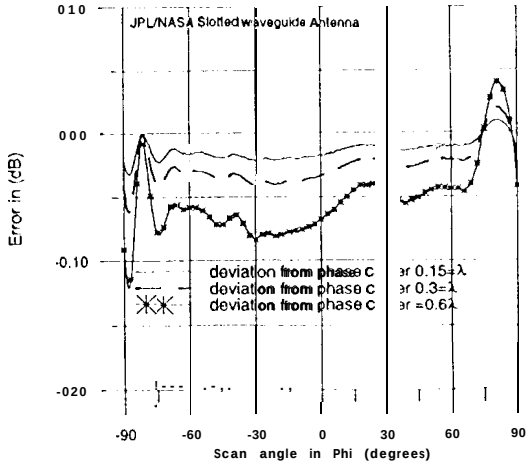

Figure 4. Typical far-field pattern error variation due to lack of accurate knowledge of separation distance between antenna under test and phase center location.

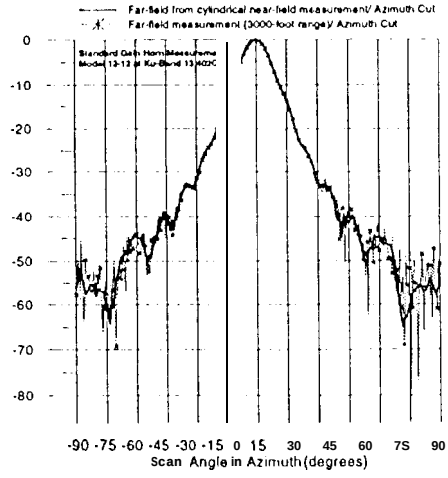

Figure 5. Comparison of standard gain horn far-field pattern obtained from cylindrical near-field measurement and direct far-field measurement.

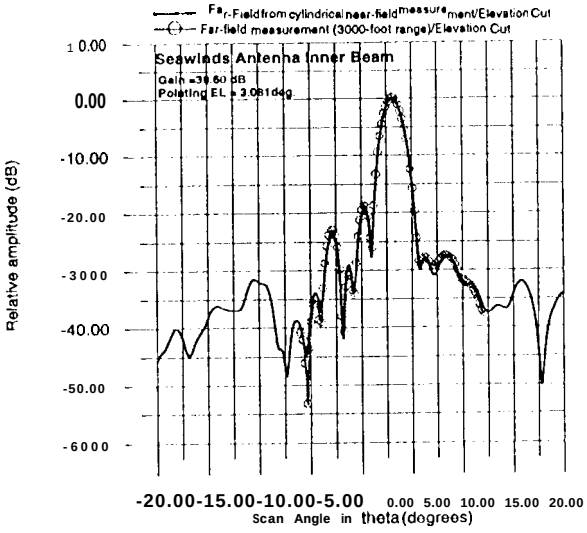

Figure 6. Comparison of H-pol SeaWinds radar antenna elevation plane far-field pattern obtained from cylindrical near-field measurement and direct far-field pattern measurement.

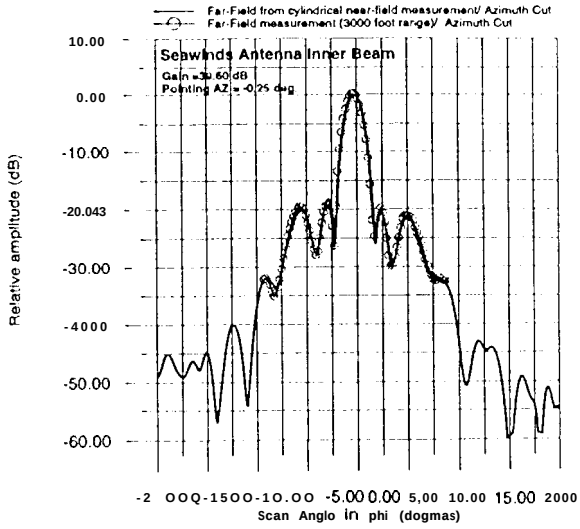

Figure 7. Comparison of H-pol SeaWinds radar antenna azimuth plane far-field pattern obtained from cylindrical near-field measurement and direct far-field pattern measurement.

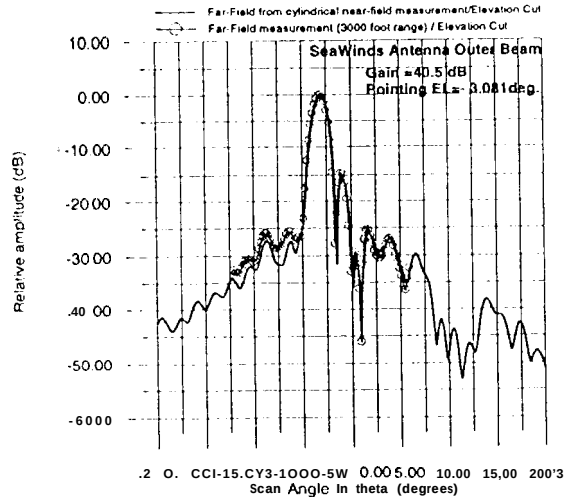

Figure 8. Comparison of V-pol SeaWinds radar antenna elevation plane far-field pattern obtained from cylindrical near-field measurement and direct far-field pattern measurement.

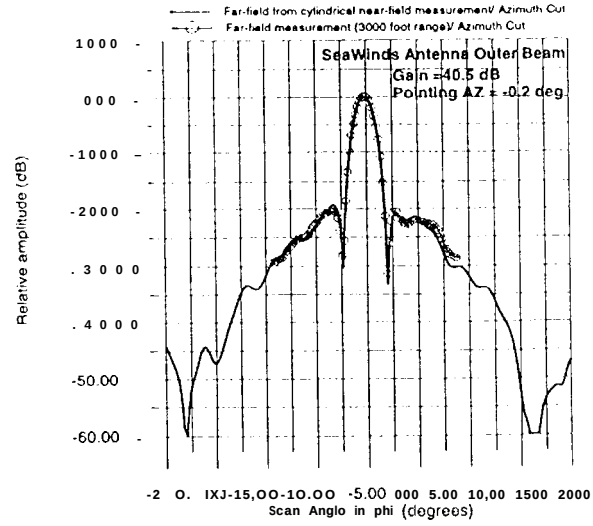

Figure 9. Comparison of V-pol SeaWinds radar antenna azimuth plane far-field pattern obtained from cylindrical near-field measurement and direct far-field pattern measurement.